I. THE ORIGIN OF THE VES HYPOTHESIS

Many processes in biology are powered by the hydrolysis of adenosinetriphosphate (ATP). Examples are muscle contraction, active transport across membranes, DNA repair and chaperone action in protein folding. In all these cases, an energy of approximately 0.45 eV is released at the active site, where the chemical reaction takes place, and must then travel to other regions of the proteins, where it is used for work. In spite of all the progress that has been made in the knowledge of those processes, the mechanism by which such a relatively small amount of energy escapes dissipation into heat before it is transformed into useful work, remains largely unknown. The possibility that vibrational excited states (VES) are involved (the VES hypothesis [15]) was first put forward by Colin McClare in the early 1970's (see [69] for McClare's seminal contribution and [91] for a tribute to him and more of McClare's references). At the time, there was not much enthusiasm for McClare's "excimers" (his designation for vibrational resonance between excited states), the main objection being that the lifetime of vibrational excited states, thought to be typically in the subpicosecond timescale, was too short for VES to be useful [70].

Davydov, a Ukrainian solid state physicist, took up McClare's suggestion that that the carrier of the energy of hydrolysis of ATP is the amide I excitation (essentially a stretching of the C=O bond of the peptide groups) and applied to its motion a Hamiltonian very similar to that which describes an electron in a polarizable crystal [53]. From his analytical studies [33, 34, 36], Davydov concluded that, just as happens in the case of the polaron, the amide I vibration induces a local compression in the hydrogen bonded chains that stabilize protein α-helices which in turn localizes the quantum vibration. This self-trapped state constituted by a localized the amide I vibration with its correlated lattice contraction is known as the Davydov soliton. Davydov thought that the known stability of soliton solutions ensured a greater lifetime for the amide I vibration and thus solved the first objection to the VES hypothesis.

While Davydov's studies were made within a continuum approximation, Scott, one of the pioneers of nonlinear science, took an interest in this problem and, together with co-workers, made the first simulations in the full discrete system [57, 66, 83, 84]. The general conclusion

was that, for the parameter values that are associated with proteins, the Davydov soliton can arise and are dynamically stable in the full discrete system. A first surprise was that, in the discrete system, solitons only form above a threshold value for the interaction between the amide I and the hydrogen-bonded lattice (we shall come back to this point in sections III and IV).

All studies mentioned so far were performed in the absence of a thermal bath. However, proteins work at finite temperature and thus, around the middle 1980's, the question of the thermal stability of the Davydov soliton arose. Davydov's own analytical work on a continuum medium indicated that the effect of temperature was to broaden the soliton, so that, at biological temperatures the amide I state would be broader than at zero temperature, but still localized and stable [35, 37]. On the other hand, the first simulations in which a *classical* bath was added to the zero temperature equations in the full discrete system predicted that, at biological temperature, the Davydov soliton was *not* thermally stable and could disperse in a few picoseconds [63]. Although many researchers then concluded that the Davydov/Scott model cannot be used to explain energy transfer in proteins [60, 61, 63], we shall see in sections V and VI that the matter is in fact not closed yet.

In a broader context, the interest in the possible role of quantum states in Biology has been re-kindled by recent experiments that demonstrate the existence of long-lived quantum coherences in systems like the light harvesting complexes [52, 56, 73, 74]. Also, other possible roles for quantum excitations in Biology have been proposed within olfaction [46, 90], bird navigation [80] and anesthesia [92]. While all the latter examples involve electronic excitations, the aim of this work is to review the state of the art of the Davydov/Scott model for vibrational energy transfer in proteins and its possible implications for the protein conformational changes. In section II the Davydov/Scott Hamiltonian is introduced and the equations of motion are derived, within the mixed quantum-classical approach according to which the hydrogen-bonded lattice moves as a classical system. In section III exact minimum energy states are obtained and the dependence of the amide I band on the lattice configuration is investigated. In section IV the different classes of dynamical solutions at zero temperature are explored. In section V the effect of adding a classical bath to the Ehrenfest equations is described and the limitations of this approach are pointed out. In

section VI a set of equations capable of reproducing the correct canonical ensemble of a mixed quantum-classical system is used to predict the finite temperature dynamics of the amide I excitation in a hydrogen-bonded chain. In section VII the possibility that VES can trigger a specific protein conformational change is tested and in section VIII the ideas and results presented in this work, and a general evaluation of the status of the Davydov/Scott model is made.

II. THE DAVYDOV/SCOTT HAMILTONIAN

The two main secondary structures of proteins, α-helices and β-sheets, are maintained by hydrogen-bonded chains with the following chemical structure:

$\cdots$ H-N-C=O $\cdots$ H-N-C=O $\cdots$ H-N-C=O $\cdots$

where H-N-C=O is the peptide group and the dots indicate the hydrogen bonds between them. Here we shall consider the motion of the amide I (a normal mode of the peptide group essentially constituted by the stretching of the C=O bond) in this hydrogen bonded chain. The sites in the lattice are thus the peptide groups H-N-C=O and the amide I vibration is an internal mode of these sites. In such a one dimensional lattice, the Davydov/Scott Hamiltonian includes three terms:

$$\hat{H} = \hat{H}_{\rm ex} + H_{\rm ph} + \hat{H}_{\rm int} \tag{1}$$

where $\hat{H}_{\rm ex}$, the exciton Hamiltonian, describes the storage and propagation of amide I excitations, $H_{\rm ph}$, the phonon Hamiltonian, describes the motions of the lattice sites and $\hat{H}_{\rm int}$, the interaction Hamiltonian, describes the interaction between the amide I excitations with the lattice. While the motion of the lattice sites is treated classically, the amide I excitations are treated quantum mechanically, something that is signalled by the hats over $\hat{H}_{\rm ex}$ and $\hat{H}_{\rm int}$.

Considering only nearest neighbour interactions, the exciton Hamiltonian is:

$$\hat{H}_{\rm ex} = \epsilon \sum_{n=1}^{N} \hat{a}_n^\dagger \hat{a}_n + J \sum_{n=1}^{N} \left(\hat{a}_n^\dagger \hat{a}_{n-1} + \hat{a}_{n-1}^\dagger \hat{a}_n \right) \tag{2}$$

where ϵ is the energy of an amide I excitation, assumed to be the same at all sites, $\hat{a}_n^\dagger$ ($\hat{a}_n$) is the creation (annihilation) operator for an amide excitation in site n and J is the interaction between amide I vibrations at neighbouring sites.

The phonon Hamiltonian is:

$$H_{\rm ph} = \frac{1}{2}\,\kappa \sum_{n=1}^{N} (u_n - u_{n-1})^2 + \frac{1}{2\,M} \sum_{n=1}^{N} p_n^2 \tag{3}$$

where κ is the elasticity of the lattice (in this case, approximately given by the elasticity of a hydrogen bond), u_n is the displacement from equilibrium position of lattice site n, M is the mass of each site (assumed to be equal for all sites) and where only small oscillations around the equilibrium positions are considered so that the motions of the lattice sites can be described by a harmonic term.

Finally, the interaction Hamiltonian is:

$$\hat{H}_{\rm int} = \chi \sum_{n=1}^{N} (u_{n+1} - u_{n-1})\ \hat{a}_n^\dagger \hat{a}_n \tag{4}$$

where χ is the change in amide I excitation with a change in the hydrogen bond length.

Exact treatments of the full quantum Davydov/Scott model, in which the lattice displacements and momenta are treated as operators, have been considered in very few cases [29, 95]. Indeed, the equilibrium regime of the full quantum system can be studied, in an exact manner, by Quantum Monte Carlo methods, the only practical limitation being the availability of sufficiently powerful computers. On the other hand, the dynamics of the full quantum system always requires approximations either in the wavefunctions or in the equations of motion (see e.g. [76, 77, 94]). As it is in fact quite difficult to evaluate the degree of accuracy of a trial wavefunction, a different approach is adopted here which consists in assuming that the motion of the lattice sites can be treated classically. This should not be confused with the adiabatic approximation, used by Davydov [33, 34, 36], in which the kinetic energy of lattice sites is neglected, something that is *not* done here. In fact, once this single assumption is made (that the lattice behaves classically) it is possible to write the *exact* wave function for one quantum of amide I excitation, in a site basis, as:

$$|\psi> = \sum_{n=1}^{N} \varphi_n\,(\{u_n\}, \{p_n\}, t)\ \hat{a}_n^\dagger |0> \tag{5}$$

where $|0>$ is the vacuum state for the amide I excitations and where correlations between the amide I and the lattice are included because φ_n, the probability amplitude for an amide I excitation to be in lattice site n, is dependent on the lattice variables in a way that will

be determined by the equations of motion.

The advantage of the mixed quantum-classical approach followed here is that the accuracy of all results is only dependent on the validity of the assumption that the motion of the lattice sites can be treated classically. The validity of this assumption for the Davydov/Scott model has been tested in the equilibrium regime. It was found that, at 0.7 K, the lattice displacement correlated with the position of the quantum particle in exact mixed quantum-classical Monte Carlo simulations differed by 15 % from the corresponding variable in exact full quantum Monte Carlo simulations and that, at 11.2 K, the two approximations lead to virtually the same value [28].

Substituting (5) in the Schrödinger equation for the amide I excitation and from Hamilton's equations for the functional (6):

$$\mathcal{E} =< \psi|\hat{H}|\psi >= \mathcal{E}\left(\{\phi_n\},\{u_n\}\right) \tag{6}$$

while making use of the Hellmann-Feynman theorem (see e.g. [89], p.298), we derive the following Ehrenfest equations of motion:

$$\begin{aligned} \imath\hbar\frac{d\varphi_n}{dt} &= \left[\epsilon+\chi\ \left(u_{n+1}-u_{n-1}\right)\right]\varphi_n + \\ &\quad +J\ \left(\varphi_{n+1}+\varphi_{n-1}\right) \end{aligned} \tag{7}$$

$$\begin{aligned} M\,\frac{d^2u_n}{dt^2} &= \kappa\ \left(u_{n+1}+u_{n-1}-2\,u_n\right)+ \\ &\quad +\chi\left(|\varphi_{n+1}|^2-|\varphi_{n-1}|^2\right) \end{aligned} \tag{8}$$

Re-scaling the time t and the displacement variables u_n in the following way:

$$\tau=\Omega\,t,\ \Omega=\sqrt{\frac{\kappa}{M}},\ q_n=\frac{\kappa}{\chi}\,u_n, \tag{9}$$

and defining two new variables, v and m:

$$v=\frac{J}{\chi^2/\kappa},\ m=\frac{\hbar\Omega}{\chi^2/\kappa} \tag{10}$$

equations (7-8) become:

$$\begin{aligned} \imath\,m\frac{d\phi_n}{d\tau} &= \left(q_{n+1}-q_{n-1}\right)\ \phi_n + \\ &\quad +v\ \left(\phi_{n+1}+\phi_{n-1}\right) \end{aligned} \tag{11}$$

$$\begin{aligned} \frac{d^2q_n}{d\tau^2} &= \left(q_{n+1}+q_{n-1}-2\,q_n\right)+ \\ &\quad +\left(|\phi_{n+1}|^2-|\phi_{n-1}|^2\right) \end{aligned} \tag{12}$$

where $\phi_n = e^{-\frac{i}{\hbar}\epsilon t}\,\varphi_n$. Equations (11-12) show that the zero temperature dynamics of one quantum of amide I in a hydrogen-bonded lattice depends on two parameters only, namely, v and m. The former measures the amide I coupling strength with respect to its interaction with the lattice while m uses this latter interaction as a unit for the energy of a lattice vibration. The values that have been mostly used in the literature are given in the table below.

variables	values
J	8 cm^{-1}
κ	13 N/m
M	114 a.m.u.
χ	62 pN
v	0.54
m	3

In sections V and VI the dynamics at finite temperature will be discussed and T will be given in units of $\chi^2/\left(\kappa\, k_B\right)$, where k_B is Boltzmann's constant.

III. EXACT MIXED QUANTUM-CLASSICAL STATIONARY STATES

The first studies of the Davydov/Scott model were performed by Davydov, in a continuum approximation [33, 34, 36]. He looked for travelling wave solutions and obtained a nonlinear Schrödinger equation (NLSE) for the probability amplitude. The conclusion from these studies is that for any finite χ, however small, the minimum energy solution is a sech pulse [33, 34, 36]. Scott and co-workers, on the other hand, investigated the discrete lattice and found that, in a lattice, a localized solution only appears above a threshold for χ [57]. Below, it is shown that these two apparently contradictory findings can be reconciled by the fact that the threshold for χ above which there is a localized solution *decreases* as the number N of lattice sites increases [27], so that, for any finite value of χ there is a number N of lattice sites *above which* the minimum energy solution is a localized state and as $N \to \infty$, any finite value of χ, no matter how small, will lead to a localized state, as Davydov found.

One advantage of the mixed quantum-classical approach is that the minimum energy states for *any values of the parameters of the system* can be determined by minimizing the

functional $\mathcal{E}$ (6). On the other hand, one difficulty with the minimization of the functional (6) is that the variables $\{\phi_n\}$ must satisfy the nonlinear constraint $\sum_{n=1}^{N} |\phi_n|^2 = 1$ which translates the normalization condition of the wavefunction. In [26, 27] the routine E04VDF from NAGlib, which performs minimization of functionals for variables that must satisfy a nonlinear constraint, was used. Instead, here, another method, already successfully tested in [12, 30] was applied in order to avoid the nonlinear constraint. This method makes use of the fact that the minimum energy state must also be the lowest energy eigenstate of the eigenvalue problem (13) below. Thus, we start with a given set of displacements $\{u_n\}$, which should be as close as possible to the global minimum and we solve the eigenvalue problem:

$$\left(\hat{H}_{\rm ex} + \hat{H}_{\rm int}\right) |\psi >_j = E_j |\psi >_j,\ j = 1 \cdots N \tag{13}$$

We then take the normalized lowest energy eigenstate, thus automatically obeying the nonlinear constraint (to make it faster, numerical methods to obtain just this lowest eigenstate can be used). Assuming that $j = 1$ corresponds to the lowest energy, we then apply standard minimization protocols to minimize the functional $E_j\left(\{q_n\}\right) + H_{\rm ph} = \mathcal{E}'$ (in this work, the routine FRPRMN from Numerical Recipes [79] has been used for the minimization). As shown in the previous section, the behaviour of the Davydov/Scott system depends on two variables only, designated as m and v (see (10)). In particular, Eqs.(11) show that eigenstates (and thus minimum energy states) are only dependent on the v (10). Here, in calculating the dependence of the minimum energy states on v we started with $v = 0$ and increase it in steps of 0.05 and took as the displacements of minimum energy solution for previous v value as the initial condition for the minimization protocol to get the new minimum for the next, higher v value. This slow and continuous progression in v may explain why, here, localized minimum energy solutions are found for much higher values of v than in [27]. Indeed, while in [27] the transition to a delocalized minimum energy state was obtained for v below 4, here this transition takes place at $v \approx 10.45$ (see figure 1). In the early dynamical studies by Scott and co-workers [57], the threshold for soliton formation was found to be $v = 2.4$ (considering $J = 7.8$ cm^{-1}, $\kappa = 76$ N/m and $\chi = 70$ pN). However, this threshold was determined from dynamical simulations of amide I propagation in the full three dimensional α-helix, i.e. what was determined was not the minimum energy state but the value of χ above which solitons (or better, solitary waves) appear when one site in the helix is excited. It should be noted that whereas other threshold values of χ will be obtained when different

initial conditions are considered [66, 83], the threshold value for the minimum energy state to be localized is universal, i.e. it depends only on the number of sites N.

When $v = 0$, the amide I coupling between neighbouring sites is zero, and the minimum energy state is localized on one site, $\phi_{nr} = \delta_{nr}$, where r is the site where the amide I excitation is (see top right panel in figure 1) and the lattice contraction at r is maximum. Notice that in a lattice with periodic boundary conditions all sites are equivalent and the amide I excitation has equal probability of being in any site; but there is a correlation between the amide I location and the lattice contraction so that, once a site is chosen for the maximum lattice contraction, the maximum probability of finding the amide I excitation will also be at that site.

In the other extreme case, i.e. for $\chi = 0$ ($v = \infty$), the amide I excitation is not coupled to the lattice and the minimum energy state is a Bloch state in which the lattice displacements are all zero (the lattice is completely undistorted), the minimum energy amide I state is completely delocalized: $|\phi_n|^2 = 1/N$ and the total energy is $-2\,v$. One more difficulty in determining the minimum energy states for values of v intermediate between zero and infinity is that this delocalized Bloch state is a stationary state of the system *for any finite value of* v (or, equivalently, for any finite value of χ) and minimization protocols can get trapped in this *local* energy minimum and thus miss a localized *global* minimum. This happened to some of the energy minimizations performed in [27] and the conclusion from the results of figure 1 is that the threshold values of v beyond which the minimum energy state is delocalized have been underestimated in [27]. In fact, it is also possible that the threshold of v beyond which the minimum energy states are delocalized is slightly higher than the value obtained here. As the accuracy with which the total energy of the system $\mathcal{E}'$ is calculated increases, the greater the accuracy with which the threshold value of v is determined. Nevertheless, figure 1 shows that, in the mixed quantum-classical *discrete* system, for a sufficiently large v and for any finite N sites, there is a smooth transition from a localized minimum energy state for low values of v to a delocalized one for sufficiently high v, as found in [27]. The cause for this transition is that, as v increases, the localized solution becomes broader; eventually, for a certain value v, its tails it reach the boundaries and thus the wave function cannot anymore go exponentially to zero at the extremities. As the displacements q_j and probability amplitudes ϕ_j at the boundaries increase, a completely

delocalized solution (whose energy is $-2v$) will start to have a lower energy than a localized one. In a infinite system, the localized solution can have any size, and still go exponentially to zero at the tails and this transition does not take place. Indeed, in figure 3 of [27] it is shown that the threshold for the transition to a delocalized solution increases approximately linearly with the number of sites N and, as the results here show, for any given N, the transition to a delocalized minimum energy state as v increases may be even more smooth than predicted in [27]. Figure 1 shows that as v increases not only the amide I state becomes broader, as mentioned, but also the lattice distortion over the whole system, and the maximum contraction, decrease. Notice that in the bottom left plot of figure 1 the scales have been changed to show the ever so slight localization of the minimum energy state for $v = 10.30$: if the same scales as for the other three plots had been used, all the lines in the bottom left panel would have looked absolutely flat, as if all probability amplitudes $\{\phi_n\}$ were the exactly the same and equal to $1/N$ and all displacements $\{q_n\}$and displacement differences $\{q_n - q_{n-1}\}$ were zero.

Although the localized minimum energy solutions found here differ from the sech pulse solution of the NLSE, here we shall follow the usual practice in this field and designate them as Davydov soliton since, like the latter, also they consist of a localized amide I wave function correlated with a localized lattice distortion (lattice compression if $\chi > 0$ and lattice expansion if $\chi < 0$). As mentioned above, these Davydov solitons are self-trapped states equivalent to Holstein's polaron [53, 54], i.e. they arise because an attractive between the amide I excitation and the lattice leads to a distortion of the lattice which, in turn, leads to potential well that traps the amide I excitation. If we were dealing with electrons (instead of the amide I excitation) these results would correspond to going from the small polaron regime (at small v) to the large polaron regime (at larger v) to the Bloch regime for sufficiently large v. Another advantage of the mixed quantum-classical approach is that it is valid for all values of v (and m).

While minimum energy solutions have zero velocity, amide I propagation requires excited states i.e., for the dynamics it is important to know the full band of amide I states. For $v = 0$ and $N = 50$, the structure of the excited states is quite striking: the lowest energy state, displayed in top right panel in figure 1, has an energy of -0.98, the first two excited

states are degenerate (their energy is 0.04) and the next 47 excited states are degenerate as well (their energies are 1.04). The tiniest deviation of v from zero breaks the degeneracy, with proportionally small deviations in these eigen-energies, but very large changes in all excited eigenfunctions, which become similar to those obtained for $\chi = 0$ ($v = \infty$). In figure 2 the full band of amide I states is shown for different sets of displacements $\{q_n\}$ and different values of v, for a shorter lattice with $N = 10$, so that the complete band can be more easily displayed. The top left panel of figure 2 shows that, for $v = 0$, not only the minimum energy amide I state is localized, as we knew from figure 1, but also all the excited states associated with that same lattice configuration are localized. Notice however that the localization is at a different site for each of the excited states. On the other hand, the top right panel shows that while a very small value of v does not produce a significant change, either in the lowest amide I state, or in the lattice distortion, the same is not true for the corresponding excited amide I states. Indeed, all excited states of the amide I for $v = -0.000001$ are completely different from the $v = 0$ ones and much more similar to those that are obtained for higher values of v (compare them with the excited amide I states displayed in the bottom left panel which are obtained for $v = -0.54$).

For $\chi = 0$ $v = \infty$, the amide I band is constituted by delocalized Bloch states which can be obtained analytically [17, 44]:

$$\phi_{jn} = \sqrt{\frac{1}{N}} \exp\left[\frac{2\pi i j n}{N}\right] \tag{14}$$

where ϕ_{jn} is the probability amplitude for an excitation in site n in the j-th eigenstate whose energy is

$$E_j = 2\,v\,\cos\left[\frac{2\pi(j-1)}{N}\right] \tag{15}$$

where $j = 1, \ldots, N$. The excited states in the bottom left panel of figure 2, which have been calculated for $v = -0.54$, retain much of the delocalized character of these Bloch states.

The bottom right panel of figure 2 shows the amide I states that appear when the lattice is disordered, something that occurs as the temperature increases (in this panel $T = 0.5$). Comparing the amide I states in the left and right panels we see that lattice disorder leads to more localized amide I states, as would be expected from Anderson localization [4]. The binding energy of the Davydov soliton is usually estimated by the energy difference between

the lowest exciton state $-2v$ with respect to the energy of the soliton state [34, 82]. Figure 2 shows that this estimation is only approximately valid, even at zero temperature, because for finite v the first excited state differs from a Bloch state. Moreover, at finite temperature, given that the number of disordered states, such as those in the bottom right panel of figure 2, is much greater than the number of soliton and exciton states, which are one and N, respectively, it is likely that the thermal destabilization of the Davydov soliton is via disordered states like those, as first suggested in [23]. For a more detailed discussion on the dynamics of the amide I excitation at finite temperature see sections V and VI.

IV. DYNAMICS AT ZERO TEMPERATURE

As indicated by equations (11-12), the dynamics of the amide I excitation in the mixed quantum-classical approach depends on v and m. We have already seen that the parameter v determines the width of the localized solution and in this section we shall investigate mainly the influence of m on the dynamics. Of course, dynamical trajectories also depend, and rather crucially, on the specific initial conditions considered. The initial conditions that have been used in the literature range from one quantum of amide I excitation at one site [57, 60] or two [60, 66, 83] or even three sites excited [60] to discrete versions of the Davydov soliton sech pulse solution [63]. Instead, in this work, in order to look for universal behaviour and also for reasons that will become clear in section VI, we will focus on initial conditions that are eigenvectors of $\hat{H}_{\rm ex} + \hat{H}_{\rm int}$ and, in particular, on minimum energy states. At zero temperature, they are uninteresting since they do not move (this fact actually provides a very good method of checking the accuracy of the states obtained by the minimization method described in the previous section: insert the minimum energy state in Eqs. (11-12) and check that it does not move and that all three energies, in the total Hamiltonian (1), averaged over the wavefunction, remain separately constant). In order to set the amide I in motion, momenta have been added the lattice sites in the following manner:

$$p_j = A\ (q_j - q_{j-1}) \tag{16}$$

where $(\{q_j\})$ are the lattice displacements of the minimum energy states and the greater the factor A, the greater the initial momenta. In figure 3 is displayed the time evolution from such a velocity driven minimum energy state, for different values of m and A. Notice that the

symmetric of lattice contractions is plotted so that positive values of $-(q_n - q_{n-1})$ actually represent local lattice contractions and negative values represent expansions. While the unperturbed minimum energy solutions, being stationary states, would of course not change, either in their position, or in their shape, strikingly, this figure shows that adding momenta to the minimum energy solution, not only sets it in motion, but also leads to the formation of double discrete breathers (DDBs). Discrete breathers (DBs) are non-topological, spatially localized, time-periodic solutions, first identified by Sievers and Takeno [86], who designated them as intrinsic localized modes (ILMs). Later, ILMs were found to be general solutions of nonlinear lattices and became known as DBs [7, 45, 65]. Indeed, while solitons are solutions that strictly can only arise in continuum Hamiltonian systems with an infinite number of conserved quantitites, DBs share with solitons the attribute of being localized but can arise in a large variety of systems that include two ingredients: nonlinear interactions and discreteness. For recent reviews on DBs see [7, 45]. The Davydov/Scott Hamiltonian (1-4) includes two fields - the amide I, described by the variables $\{\phi_n\}$ and the lattice, described by variables $\{q_n\}$ - both of which, *by themselves*, are linear and unable to sustain DBs. The only nonlinear term in the Davydov/Scott Hamiltonian is the interaction Hamiltonian (4) which is linear in $\{q_n\}$ and nonlinear in $\{\phi_n\}$. Figure 3 shows that this nonlinear term is sufficient to generate *moving* DDBs. This designation is due to the fact not only a moving DB is observed in the lattice but also a correlated moving DB is observed in the motion of the quantum amide I excitation through the lattice. Figure 3 also shows that the larger the initial momenta, the larger the velocity with which the DDB moves but also the higher the frequency with which the DDB oscillates. On the other hand, this frequency is approximately the same for the two DBs (in the lattice and in the amide I excitation) but the amplitude of oscillation varies. Indeed, as m increases, the amplitude of oscillation of the lattice DB decreases, as does the frequency of the DDBs.

Figures 3 and 4 also reveal several destabilizing factors for DDBs. One is the emission of lattice phonons, which leads to a decrease in the amplitude of the lattice contraction (this is clearly visible in the middle plots (red) of the four panels of figure 3). A second destabilizing factor is the interaction of the phonons with the DDBs (which is visible in the middle plots of the top right and bottom panels of figure 3, while figure 4 shows that, for a sufficiently long time, in a sufficiently intense phonon field, the DDBs can be totally dissipated). A third cause of instability for DDBs is the radiation emitted by the quantum amide I state

(which is more clearly visible for the short simulations with the larger velocity (i.e. with $A = 2$ as in the top right panel of figure 3) and whose final consequence can be a totally delocalized state for the amide I excitation (as seen in the top plot (red) of the right panel of figure 4). Figure 4 also shows that a population of lattice phonons can scatter the DDB, so that it inverts its direction of motion (as seen in the left panel of this figure: the velocity of the breather first decreases, which leads to a curved trajectory and then it is reversed, so that DDB starts moving in the opposite direction!)

V. DYNAMICS AT FINITE TEMPERATURE: THE CLASSICAL LANGEVIN APPROACH

While the minimum energy solutions mentioned in section III are dynamically stable, no exact moving solutions have yet been determined for the discrete system and the simulations in the previous section already illustrate how the stability of the Davydov soliton depends on m and on the initial conditions. Davydov's idea was that the soliton, being stable, could last longer than other states and thus explain how energy can travel in a protein without dissipation [33, 34, 36]. However, as proteins perform their work at finite temperature, in the 1980's an interest about the effect of thermal baths on the soliton state grew. As mentioned above, Davydov's own analytical work on a continuum medium indicated that the effect of temperature was to broaden the soliton, so that, at biological temperatures the amide I excitation would be broader than at zero temperature, but still dynamically stable [35, 37]. On the other hand, researchers working with discrete lattices sought to investigate the effect of temperature by transforming equation (12) into a Langevin equation, and finding the evolution of the quantum amide I from the following set of equations [60, 63]:

$$\imath\, m\frac{d\phi_n}{d\tau} = (q_{n+1} - q_{n-1})\ \phi_n + \tag{17}$$
$$+v\ (\phi_{n+1} + \phi_{n-1})$$
$$\frac{d^2 q_n}{d\tau^2} = (q_{n+1} + q_{n-1} - 2\, q_n) + \tag{18}$$
$$+\left(|\phi_{n+1}|^2 - |\phi_{n-1}|^2\right)$$
$$+F_n(\tau) - \Gamma\, \frac{dq_n}{d\tau} \tag{19}$$

where the stochastic forces $F(\tau)$ and the friction parameter Γ obey the fluctuation-dissipation relation:

$$\ll F_n(\tau)\ F_m(\tau') \gg = 2\,\Gamma\,T'\,\delta_{mn}\,\delta(\tau-\tau') \tag{20}$$

where T' is related to the temperature, T by:

$$T' = \frac{k_B T}{\chi^2/\kappa} \tag{21}$$

Eqs.(17-18) were first used to investigate the thermal stability of the Davydov soliton at finite temperature by Lomdahl and Kerr [63]. They considered as initial condition a discretized version of the Davydov sech pulse [33, 34, 36] and found that, at $T = 300$ K, when $v = -0.52$ a soliton could last $100-150$ ps and when $v = -3.45$ it disperses in a few picoseconds. Figure 5 illustrates the dependence on temperature of the time evolution of the amide I state as described by eqs.(17-18). It shows that at finite temperature the Davydov soliton is not stable and disperses increasingly faster as the temperature increases. Results such as these, which contradicted Davydov's own analytical studies [35, 37], lead to a vigorous discussion in the scientific community which is summarized in [82]. As it happens, eqs.(17-18) leads to a classical behaviour, not only of the lattice, but also of the amide I excitation (see [24, 25, 29] for a full explanation and also the appendix of [47]). In short,the problem is that Eqs.(17-18) lead to a diffusion of the amide I state through the quantum phase space in a classical manner, i.e. by exploring all possible superpositions of eigenstates and, even when the eigenstates are localized, a superposition of localized states will result in a delocalized quantum state. Thus, most of the states sampled in the trajectories obtained from the integration of Eqs.(17-18) are delocalized states. These delocalized states *would* represent the correct canonical ensemble of amide I states **if** the amide I excitation *were* a classical excitation. On the other hand, as illustrated by the bottom right panel of figure 2, most of the states of a quantum vibration at finite temperature are localized and thus a correct sampling of amide I states should produce mostly localized states. Finally, notice that Eqs.(11-12) do reproduce the correct quantum behaviour of the quantum amide I excitation in a classical lattice, *at zero kelvin* and that the problem arises because the addition of a classical thermal bath to those equations. I.e., the question that remains open is how to simulate the motion of a quantum amide I excitation in a classical lattice, *at finite temperature*. In the next section, a formalism is described that preserves the classical statistics of the lattice and the quantum statistics of the amide I excitation.

VI. DYNAMICS AT FINITE TEMPERATURE: A MIXED QUANTUM-CLASSICAL FORMALISM

While the equilibrium regimes of full classical, full quantum and mixed quantum-classical systems can be investigated without approximations by Monte Carlo methods [29], the same is not true for the non-equilibrium regimes. Indeed, in the latter case, there are exact formalisms to describe the finite temperature dynamics of full classical systems, namely, Langevin equations such as (17-18) or the Nosé scheme [68, 72], and there are exact formalisms for the non-equilibrium regime of *full quantum* systems, namely, the Lindblad equation [62] and the particular case of the quantum state diffusion equation [75], but there is not yet an exact formalism to deal with the dynamics of *mixed quantum-classical* systems at finite temperature. Very often, thermal baths are added to the zero temperature equations of mixed quantum-classical system in the same way as in (17-18), that is, by adding Langevin terms to the equations of motion of the classical variables [63, 81] and, as explained above, the usual outcome is that localized quantum states tend to become delocalized (and when the quantum eigenstates are predominantly localized this is evidence that the quantum system has started to behave classically). This is a general problem of mixed quantum-classical systems and affects electrons in a classical solvent [68] and electronic and vibrational excitations in classical lattices [24, 25, 29, 47, 59]. Partial solutions proposed to deal with it include periodically bringing the quantum system to the ground state [68] or forcing the density matrix of the system to tend to the equilibrium value via the introduction of a Lagrange multiplier in the equations of motion [59]. The first solution is valid when the energy difference between the first excited state and the ground state is much larger than thermal energy, k_BT, and the second solution can only be applied when the analytical expression of the equilibrium density matrix is known. None of those conditions are verified in the case of the present system. Thus, another set of equations of motion was proposed to deal with finite temperature dynamics in the mixed quantum-classical Davydov/Scott system

[24, 25, 29, 47], as follows:

$$E_j \phi_{nj} = (q_{n+1} - q_{n-1})\ \phi_{nj} + \tag{22}$$
$$+ v\ (\phi_{n+1j} + \phi_{n-1j})$$
$$\frac{d^2 q_n}{d\tau^2} = (q_{n+1} + q_{n-1} - 2\, q_n) + \tag{23}$$
$$+ \left(|\phi_{n+1j}|^2 - |\phi_{n-1j}|^2\right)$$

Eqs.(22-23) are valid when the quantum excitations adapt infinitely fast to changes in the classical environment and avoid the sampling of superpositions of eigenstates by coupling the *stationary* Schrödinger equation for the amide I excitation to the Langevin equations of motion of the lattice sites. They thus generate the correct quantum statistics for the amide I, while, at the same time, reproducing the classical statistics for the classical lattice.

It is important to understand how these equations are integrated. An initial lattice state, defined by a set of displacements $\{u_n(t_0)\}$ and a set of momenta $\{p_n(t_0)\}$ is chosen. Using $\{u_n(t_0)\}$, the eigenvalue problem set by Eqs.(22) is solved and an eigenstate for amide I given by the probability amplitudes ϕ_{nj} is selected. This initial condition is inserted in Eqs.(23) and the displacements and momenta of the system are advanced one time step by integration of these equations. The new displacements are substituted in Eqs.(22) and a new eigenvalue problem is solved. This leads to N possible eigenstates j from which one, j', must be selected. A Metropolis Monte Carlo step is used to select eigenenergies (and thus eigenstates) according to the Boltzmann distribution. In order to prevent quantum jumps between lattice sites that may be too far apart, the overlap between the initial state and the final state (a Franck-Condon factor) is also considered in the Monte Carlo step. If $j' \neq j$, then we have a quantum jump between two Born-Oppenheimer surfaces, if not, the amide I state evolves on the same Born-Oppenheimer surface. Whether there is a quantum jump or not, there may be a jump of the amide I excitation *in real space* because the new quantum eigenstate selected may have a maximum probability to be at a different site. Large jumps in real space are however prevented by the including the Franck-Condon factor.

Before applying Eqs.(22-23) to the finite temperature regime it is worth to explore their predictions at zero temperature. Figure 6 shows the time evolution of a minimum energy function with same extra velocities as in Figure 3. We see that the lowest values of m used in

Figure 3 lead to a time evolution very similar to that of Figure 6. This is because Eqs.(22-23) are valid when the amide I excitation adapts infinitely fast to the changes in the lattice, i.e., when $m \approx 0$. For this value of v, $m = 0.45$ in Eqs.(11-12) leads to a time evolution close to that situation. In fact, Eqs.(22-23), at zero temperature, lead to the most stable moving DDBs, as can be asserted from the comparative lack of radiation in the top plots of Figure 6.

The time evolution of an amide I excitation at three increasing temperatures, as predicted by Eqs.(22-23), is displayed in Figure 7. At low temperatures and for a low level of disorder in the lattice, moving DDBs can survive, as seen in the left panel of figure 7. At higher temperatures, quantum jumps (either between Born-Oppenheimer surfaces or just between lattice sites, as discussed above) of the amide I excitation are observed which drag the lattice compression with them. Figure 7 also shows that the rate of jumps increases with temperature and that, at biological temperatures ($T = 14$ with the parameters in table of section II corresponds to 310 K), the amide I states are localized and hop from one site to another much like a Brownian particle, similar to what was first obtained for the motion small polaron at finite temperature, in a perturbation approach [54]. The conclusion is that, at finite temperature, the amide I states share with the Davydov soliton the fact that they are localized, but greatly differ from it in that they hop stochastically from site to site.

VII. HOW A VES CAN GENERATE A PROTEIN CONFORMATIONAL CHANGE

Protein work is often associated with conformational changes characterized by the concerted motion of large groups of atoms [49, 50]. In most cases only the initial and final conformations of a given protein are known and the usual models consist in trying to identify, in the classical protein trajectories, one or more collective modes that can take a protein from a given initial conformation to a specific final one [3, 6, 55, 58, 67, 71]. In spite of the nonlinear character of potential energy functions used in atomistic molecular dynamics [11, 14, 64], normal modes are sometimes used [58, 67], but also the more anharmonic essential modes [3, 6] and functional modes [55, 71] have also been applied. Here, instead, the perspective is that conformational changes are triggered by vibrational excited states (the VES hypothesis) [16, 18–20]. As seen in the previous section, vibrational excited states are localized and hop stochastically from site to site, in a one dimensional lattice at finite

temperature. Generalizations of the Davydov/Scott model to proteins, taking into account their atomic structure, have shown that the amide I motion in proteins, at biological temperatures, also consists of a random hopping of a localized state from one peptide group to another in its vicinity [15, 16, 18, 19]. Thus, in this section a preliminary investigation about how a specific conformational change can be the result of a local action is reported.

The first issue to decide is what will the local action consist of? While the amide I propagation is a quantum event, the conformational change, which results from the motion of a large number of atoms, is a classical event. Thus, the initial condition for a conformational change is a set of positions and momenta for all the atoms in the protein. Below are stated what the initial positions will be. As to the momenta, it will be assumed that the decay of the amide I excitation leads to the breaking of the hydrogen bonds of the C=O groups where the amide I excitation happens to be located at the time decay takes place. In sections III-VI it was to shown that the Davydov/Scott model can explain the propagation, without dispersion or dissipation, of relatively small amounts of energy from one region of a protein to another. However, the vibrational excited states that are the carriers of this energy have a finite lifetime, probably in the picosecond timescale [38]. After that time, those states decay. The Davydov/Scott model conserves the number of amide I quanta and cannot describe this decay. A generalization of the Davydov/Scott model in which the number of amide I quanta is not conserved has been proposed in order to investigate the classical (conformational) states that are generated in the protein when the quantum amide I excitations decay. However, the non-conservation terms that were added resulted more often in the creation of amide I quanta rather than in their annihilation [87, 88]. Thus, there is not at present any knowledge about the protein states that follow the decay of amide I excitations. It is not, however, unreasonable to assume that their energy is transferred to the momenta of the C=O groups where the quantum excitation was originally localized, producing as a result an opening of those hydrogen bonds. Indeed, another study of a non-conservative Davydov monomer predicted that the amide I excitation leads to excited states of the hydrogen bond, whose memory remains long after the the amide I excitation has decayed [78].

In order to keep complexity to a minimum, a small all-α protein with just 60 amino acids

and 692 atoms was selected, namely, PDB2HEP [5]. Its native structure, obtained from the Protein Data Bank [9], and energy minimized with the AMBER force field [14], is displayed in middle panel of figure 8. On the left panel is the same protein but with the form of an α-helix. The conformational change we want to reproduce is the hinge motion which takes the protein from an initial helical structure to the final native state. In particular, we wish to generate this conformational change by breaking 1-2 local hydrogen bonds in the helix. After many trials, varying the locations for the initial breaks in the hydrogen bonds, varying the number of hydrogen bonds broken and varying the strength of the initial momenta, a set of initial conditions did lead to a structure similar to the native, as shown in the right panel of figure 8 (compare it with the native structure seen in the middle panel of the same figure). This final structure will be designated as alternative structure. The hydrogen bonds that were broken in the helix (left panel of figure 8) were the following: C=O(21)$\cdots$ H-N-C=O(25)$\cdots$ H-N(29), where in parenthesis are the amino acid numbers in the primary sequence of the protein. The direction for the initial momenta in those groups was along the hydrogen bond O $\cdots$ H and in a sense in each atom to open that hydrogen bond. The initial velocities were the same in the C and O atoms and in the H and N atoms, respectively. The velocities of the other atoms of the protein were taken from a Maxwell-Boltzmann distribution at $T = 298$ K. As Langevin terms, like those of equations (18) and (23), eliminated the effect of the initial momenta, apart from the thermal initial velocities, the simulations reported here were all made in the microcanonical ensemble (option NTT=0, in the AMBER package [14]).

At 298 K, proteins fluctuate within a local basin of attraction. It is important to compare the stability of the alternative structure obtained (right panel of figure 8) with that of the native state (middle panel of the same figure). The root mean square deviation (RMSD) of each conformation with respect to the average structure was taken as a measure of the degree of fluctuation of the two conformations and is displayed in figure 9. This figure shows that the degree of fluctuation of the two conformation is of the same order of magnitude, with the alternative structure being actually *less* flexible than the native.

For the localized initial push explored here to be a viable way of generating conformational changes, it should not depend on the thermal velocities of the other atoms in the protein.

Thus, more simulations were performed in which the initial structure was always the α-helix in the left panel of figure 8 and in which the initial velocities in C=O(21)...H-N-C=O(25)...H-N(29) were kept the same as for the alternative structure (right panel of figure 8) but the velocities in the other atoms were changed (but still selected from a Maxwell-Boltzmann distribution at $T = 298$ K). Again, the RMSD was used as an estimate of the structural difference between two conformations. In this case we are interested in the effectiveness with which the same initial push described above (together with different thermal velocities in the other atoms) leads to the native structure and the RMSD values of each structure sampled in the trajectory with respect to the native structure are displayed in figure 10. The trajectories with initial pushes are represented in blue (generally lower curves in figure 10) and the trajectories without initial pushes and just thermal velocities in all the atoms are represented in red (the top curves in figure 10). In broad terms, three types of outcomes were obtained: 1) those trajectories in which the pushes lead to structures within 6 Å of the native, as the structure in the right panel of figure 8 (blue curves in the top panel of figure 10); 2) those trajectories in which the pushes lead to structures within 9 Å of the native (blue curves in the middle panel of figure 10) and 3) those trajectories in which the pushes lead to structures more than 12 Å away from the native (blue curves in the bottom panel of figure 10). We find that 20% of the trajectories are of type 1); 40% of the trajectories are of type 2) and another 40% of the trajectories are of type 3). On the other hand, in the absence of an initial push, and with the just same thermal initial velocities that had been used for the trajectories with the pushes, *none* of the trajectories shows any sign of the α-helix to evolve towards the native state. This is in stark contrast to the trajectories with the pushes which, even when they do not achieve the native state, always show some tendency to evolve to it. Thus, the conclusion is that, although the goal of defining initial conditions that are sufficient to achieve the native state has clearly not been achieved, figure 10 does show that inducing local breaks in the hydrogen bonds between the peptide groups in a protein *can* make it more likely for the α-helix to evolve towards the native state.

VIII. DISCUSSION AND CONCLUSION

The status of the Davydov/Scott model for vibrational energy transfer in proteins, in the mixed quantum-classical approach, was reviewed. In a discrete lattice, for a sufficiently

strong amide I-lattice interaction, χ, it is known that the exact the minimum energy state is constituted by a localized amide I excitation correlated with a local lattice contraction (the Davydov soliton). In section III it was shown that the threshold value of χ above which the minimum energy states are localized is smaller than previously thought [27]. Furthermore, in section IV, new states were found when minimum energy states are velocity driven, in which both the amide I and the lattice sites move as breathers, (designated as DDBs). While there a number of reports of solito-breathers [30, 31] and polaro-breathers [32] in systems in which quantum particles move in a *nonlinear* lattice, the observation of these types of solutions in lattices which, when isolated, are harmonic is comparatively rare [93]. In fact, I am not aware of another report of *moving* breathers, such as the DDBs reported in section IV, in the latter kind of systems.

While most of the attention of the scientific community in this area has been focussed on the Davydov soliton and its stability, a more pertinent question is whether solitons *can* arise in structures that lack any kind of symmetry and which are as dynamically disordered as proteins. Indeed, although the perfect α-helix does possess helical symmetry [10, 42, 43] (see the left panel of figure 8), at biological temperatures their structures are irregular (see the middle and right panels of figure 8). In such disordered structures many Anderson localized states, rather than the soliton, can be populated which are at least equally capable of transferring, without dispersion or dissipation, the approximately 0.45 eV of energy released in the hydrolysis of ATP, from the active sites to other regions of a protein where this energy is needed for work. In fact, while solitons have a defined direction of motion and will be blocked if a mutation occurs in one part of their path, the Anderson localized states that hop stochastically from one protein site to another (see section VI) may still be able of finding alternative paths for energy transfer. The proposal here is that, at biological temperatures, Anderson localized states are the carriers of the amide I excitation.

It was also shown how the investigation of the thermal stability of the Davydov soliton eventually lead to a deeper question of how to correctly simulate the non-equilibrium finite temperature dynamics of a mixed quantum-classical system [24, 25, 29]. Indeed, the procedure that is commonly applied to thermalize the latter systems, which consists of adding a classical bath to the zero temperature equations of the classical variables of

the system (see [60, 61, 63] and section V), leads to a classical behaviour of the quantum particle [24, 25, 29, 47]. In spite of several remedial suggestions [24, 29, 47, 68, 81], an exact answer to this question has not yet been found. Thus, curiously, at present, while exact formalisms exist to describe the finite temperature dynamics of either fully quantum systems [62, 75], or of fully classical systems [29, 72], mixed quantum-classical systems remain as the most difficult to deal with (of course, in practice, fully quantum systems are also rather awkward because, even if formalisms exist, the quantum (Lindblad) operators that describe the action of the bath are only known in an exact manner for quantum harmonic oscillators).

In the context of the previous paragraph it is important to point out several limitations of Eqs.(22-23) for the finite temperature dynamics of the mixed quantum-classical Davydov/Scott model. While those equations are correct in the sense that, when integrated for a sufficiently long time, they can reproduce the canonical ensemble of the mixed quantum-classical system, a first limitation is that they are only strictly valid when the quantum particle (the amide I excitation) responds infinitely fast to the changes in the lattice configuration [29]. A second strong limitation is that, because only eigenstates of the quantum particle are considered, the parameter m (see (10)) does not influence the dynamics. As m is the only parameter that depends on the mass of the lattice sites, Eqs.(22-23) cannot deal with isotopic effects, which is one of the ways the quantum nature of a system manifests itself. A third limitation is that superposition of eigenstates are never sampled and thus phenomena like coherence/decoherence cannot be investigated with Eqs.(22-23). Finally, a fourth limitation is the validity of the mixed quantum-classical approach itself, i.e., is the motion of the protein sites classical at finite temperature? I would say yes. In fact, that is the assumption made in the vast majority of molecular dynamics simulations of proteins [3, 6, 15, 16, 18–20, 47, 55, 58, 67, 71].

A crucial question for any model is whether there is experimental evidence for it. In [82] a description is made of the early experiments on the effect of electromagnetic fields on cell growth, which was first interpreted as evidence for the role of Davydov solitons in biological systems, as well as of the reasons for why that evidence was later dismissed. Currently, the best evidence for a self-trapped, Davydov soliton-like, amide I state in chains of hydrogen bonded amide groups is thought to be the amide I band the organic crystal of acetanilide

(ACN) [13, 38–40]. Indeed, the spectral measurements by Careri and co-workers showed that when crystalline ACN is cooled, a new, anomalous, peak arises, which is red-shifted by approximately 16 cm^{-1} with respect to the conventional main peak at 1666 cm^{-1}, and whose intensity increases as temperature decreases [13]. The current theories, which were first put forward in the 1980s [1, 2, 13, 41, 82, 85], propose that the conventional, higher energy, peak corresponds to delocalized, Bloch exciton states and that the anomalous, lower energy, peak is due to self-trapped states of the amide I excitation. Nonlinear spectroscopic measurements, in which a finite nonlinear response is interpreted as a signature anharmonic, self-trapped states provided further confirmation for those interpretations [38, 39]. However, recent theoretical calculations of the full amide I band of crystalline ACN, which take into account the complete atomic constitution of the crystal, are able to reproduce the temperature double peak structure of crystalline ACN without resorting to self-trapped states [21, 22]. In the latter calculations, the conventional higher energy peak is due to weakly-hydrogen bonded or unbonded C=O groups and the lower energy peak is due to strongly bonded C=O groups, both of which arise from thermal agitation, *in the absence of amide I excitations* [21, 22]. I.e. Anderson localized states (see bottom left panel of figure 2) alone are able to explain the structure of the amide I band of crystalline ACN.

The recent experimental measurements [38–40] have however re-introduced the old problem of the duration of an amide I excitation. Indeed, measurements in crystalline ACN suggest that the lifetime of an amide I excitation is a few picoseconds [38] and not much higher in the protein myoglobin [8, 96]. Thus, one important question is whether a lifetime of a few picoseconds is enough for the amide I to be useful energy carrier in proteins? According to the simulations mentioned in sections VI and VII, we would say yes. Indeed, those simulations indicate that it takes only a few picoseconds for an amide I excitation to travel from the active site to any other protein site. Also, according to the simulations in section VII, its decay into classical hydrogen bond breaking modes can lead to a well defined conformational change, in the nanosecond timescale. Whereas Davydov [33] envisaged a change in the protein concomitant with soliton propagation, which would only be viable if protein work (in Davydov's case, muscle contraction) occurred in the picosecond timescale, the perspective here is that the amide I's role is simply to carry the energy within the protein in a form that prevents it from disappearing into heat. This role does

not require a soliton state but does require a quantum state that is well separated from the many classical dissipative modes in a protein. Eqs.(22-23) predict that the quantum amide I states are localized at biological temperatures and thus raise the question of how a local quantum energy input can lead to the concerted motion of a large group of atoms that characterizes conformational changes. In section VII the hypothesis that the decay of the quantum state leads to the break of hydrogen bonds between the C=O groups where amide I excitation happens to be located is considered. Simulations were thus made to test whether a local break of that type of hydrogen bonds in a protein can indeed lead to a specific conformational change, namely, a hinge motion in a small protein. Although they cannot be considered definitive proof by any means, the preliminary simulations reported in section VII identified one case in which the breaking of 1-2 local hydrogen-bonds leads to a specific conformational change, with some degree of reproducibility.

The conformational changes in section VII take place in the nanosecond timescale, some 2 to 3 orders of magnitude longer than the picosecond time scale of quantum amide I propagation (see section VI), but still much faster than the time scale of most protein mediated processes in cells, which can be microseconds or milliseconds or even seconds. The idea here is that those longer timescales correspond to a relaxation of protein structures, such as the alternative structure in the right panel of figure 8, to the bottom of the local free energy minimum associated with that conformation. This slow relaxation from a higher (free) energy structure, which was reached in the nanosecond time scale, as a result of a push in a specific direction of the conformational space, can explain why muscle contraction (and many other processes, such protein folding) take milliseconds, or longer, to occur. In this picture, although the quantum energy transfer is very fast (picoseconds), and the conformational change is also fast (nanoseconds), they are the defining steps in the overall, much longer, process.

In spite of the fact that the experimental evidence for the Davydov/Scott model for energy transfer in proteins remains slim, to my knowledge, that model is still the best *theoretical* candidate for an explanation of how a relatively small amount of energy can travel along a protein without being dissipated on the way and the news of its demise [8, 51, 60, 61, 63] is slightly exaggerated. While the simulations of both the full classical equations, Eqs.(17-

18), and the mixed quantum-classical equations, Eqs.(22-23), do indicate that the Davydov soliton is not stable at biological temperature, the point we wish to make is that the status of the Davydov *model* should not be equated with that of the Davydov *soliton*, as is often done [8, 51, 60, 61, 63]. Regarding future experiments, perhaps an even more basic question is which vibrational excited states are created when ATP is hydrolysed. For instance, do amide I states arise when ATP is hydrolysed? Since the theoretical description of a chemical reaction catalysed by a protein constitutes a very hard subject [48], this question should be addressed experimentally. Finally, it should be said that although the focus here is on energy transfer in proteins (and its possible consequences to protein conformational changes), the Hamiltonian (1-4) is formally similar to that used to describe electrons in polarizable crystals [53, 54] and many of the results in sections III-VI may be of interest to solid state physicists as well.

ACKNOWLEDGMENTS

This work received national funds from FCT - Foundation for Science and Technology, Portugal, through the project UID/Multi/04326/2013. The author also acknowledges the Laboratory for Advanced Computing at University of Coimbra (http://www.lca.uc.pt) for providing HPC computing resources that have contributed to the research results reported within this paper.

---

[1] Alexander, D. M. (1985). Analog of small holstein polaron in hydrogen-bonded amide systems. *Phys. Rev. Lett.*, **54**, 138–141.

[2] Alexander, D. M. and Krumhansl, J. A. (1986). Localized excitations in hydrogen-bonded molecular crystals. *Phys. Rev. B*, **33**, 7172–7185.

[3] Amadei, A., Linssen, A., and Berendsen, H. (1993). Essential Dynamics Of Proteins. *Proteins Struc. Func. Gen.*, **17**(4), 412–425.

[4] Anderson, P. W. (1958). Absence of Diffusion in Certain Random Lattices. *Phys. Rev.*, **109**(5), 1492–1505.

[5] Aramini, J., Sharma, S., Huang, Y., Swapna, G., Ho, C., Shetty, K., Cunningham, K., Ma, L., Zhao, L., Owens, L., Jiang, M., Xiao, R., Liu, J., Baran, M., Acton, T., Rost, B., and Montelione, G. (2008). Solution nmr structure of the sos response protein ynzc from bacillus subtilis. *Proteins*, **72**, 526–530.

[6] Arcangeli, C., Bizzarri, A., and Cannistraro, S. (2001). Concerted motions in copper plastocyanin and azurin: an essential dynamics study. *Biophys. Chem.*, **90**(1), 45–56.

[7] Aubry, S. (2006). Discrete Breathers: Localization and transfer of energy in discrete Hamiltonian nonlinear systems. *Physica D*, **216**(1 SPEC. ISS.), 1–30.

[8] Austin, R. H., Xie, A., Fu, D., Warren, W. W., Redlich, B., and van der Meer, L. (2009). Tilting after Dutch windmills: probably no long-lived Davydov solitons in proteins. *J. Biol. Phys.*, **35**(1), 91–101.

[9] Berman, H., Westbrook, J., Feng, Z., Gilliland, G., Bhat, T., Weissig, H., Shindyalov, I., and Bourne, P. (2000). The protein data bank. *Nuc. Acid. Res.*, **28**, 235–242.

[10] Brizhik, L., Eremko, A., Piette, B., and Zakrzewski, W. (2004). Solitons in alpha-helical proteins. *Phys. Rev. E*, **70**(3), 031914.

[11] Brooks, B. R., Brooks, III, C. L., Mackerell, Jr., A. D., Nilsson, L., Petrella, R. J., Roux, B., Won, Y., Archontis, G., Bartels, C., Boresch, S., Caflisch, A., Caves, L., Cui, Q., Dinner, A. R., Feig, M., Fischer, S., Gao, J., Hodoscek, M., Im, W., Kuczera, K., Lazaridis, T., Ma, J., Ovchinnikov, V., Paci, E., Pastor, R. W., Post, C. B., Pu, J. Z., Schaefer, M., Tidor, B., Venable, R. M., Woodcock, H. L., Wu, X., Yang, W., York, D. M., and Karplus, M. (2009). Charmm: The biomolecular simulation program. *J. Computat. Chem.*, **30**, 1545–1614.

[12] Cantu Ros, O. G., Cruzeiro, L., Velarde, M. G., and Ebeling, W. (2011). On the possibility of electric transport mediated by long living intrinsic localized solectron modes. *Eur. Phys. J. B*, **80**(4), 545–554.

[13] Careri, G., Buontempo, U., Galluzzi, F., Scott, A. C., Gratton, E., and Shyamsunder, E. (1984). Spectroscopic evidence for Davydov-like solitons in acetanilide. *Phys. Rev. B*, **30**(8), 4689–4702.

[14] Case, D., Cheatham, T. I., Darden, T., Gohlke, H., Luo, R., Merz, K. J., Onufriev, A., Simmerling, C., Wang, B., and Woods, R. (2005). The amber biomolecular simulation programs. *J. Computat. Chem.*, **26**(16), 1668–1688.

[15] Cruzeiro, L. (2005a). Influence of the nonlinearity and dipole strength on the amide I band of protein α-helices. *J. Chem. Phys.*, **123**, 234909.

[16] Cruzeiro, L. (2005b). Why are proteins with Glutamine- and Asparagine-rich regions associated with protein misfolding diseases? *J. Phys: Condensed Matt.*, **17**, 7833–7844.

[17] Cruzeiro, L. (2008a). Influence of the sign of the coupling on the temperature dependence of optical properties of one-dimensional exciton models. *J. Phys. B: Atom., Mol. Opt. Phys.*, **41**, 195401.

[18] Cruzeiro, L. (2008b). Protein's multi-funnel energy landscape and misfolding diseases. *J. Phys. Org. Chem.*, **21**, 549–554.

[19] Cruzeiro, L. (2010). Protein folding. In M. Springborg, editor, *Chemical Modelling*, volume 7 of *Specialist Periodic Reports of the Royal Society of Chemistry*, pages 89–114, London, UK. Royal Society of Chemistry.

[20] Cruzeiro, L. (2014). A kinetic mechanism for in vivo protein folding. *Bio-Algorithms and Med-Systems*, **10**(3), 117–127.

[21] Cruzeiro, L. (2015). The amide i band of crystalline acetanilide: Old data under new light. In J. F. Archilla, N. Jiménez, V. J. Sánchez-Morcillo, and L. M. Gárcia-Raffi, editors, *Quodons in Mica. Nonlinear Localized Travelling Excitations in Crystals*, volume 221 of *Springer Series in Materials Science*, pages 401–424, Heidelberg-London. Springer.

[22] Cruzeiro, L. and Freedman, H. (2013). The temperature dependent amide i band of crystalline acetanilide. *Phys. Lett. A*, **377**, 1593–1596.

[23] Cruzeiro-Hansson, L. (1992). Mechanism of thermal destabilization of the Davydov soliton. *Phys. Rev. A*, **45**, 4111–4115.

[24] Cruzeiro-Hansson, L. (1996a). Dynamics of a mixed quantum-classical system at finite temperature. *Europhys. Lett.*, **33**(9), 655.

[25] Cruzeiro-Hansson, L. (1996b). The Davydov Hamiltonian leads to stochastic energy transfer in proteins. *Phys. Lett. A*, **223**(5), 383–388.

[26] Cruzeiro-Hansson, L. (1998). Effect of long range and anharmonicity in the minimum energy states of the davydov-scott model. *Phys. Lett. A*, **249**, 465–470.

[27] Cruzeiro-Hansson, L. and Kenkre, V. (1994). Localized versus delocalized ground states of the semiclassical Holstein Hamiltonian. *Phys. Lett. A*, **190**, 59–64.

[28] Cruzeiro-Hansson, L. and Kenkre, V. (1995). Comparison of quantum Monte Carlo and semiclassical Monte Carlo results in investigations of the thermal stability of Davydov solitons. *Phys. Lett. A*, **203**(5-6), 362–366.

[29] Cruzeiro-Hansson, L. and Takeno, S. (1997). Davydov model:The quantum, mixed quantum-classical, and full classical systems. *Phys. Rev. E*, **56**(1), 894–906.

[30] Cruzeiro-Hansson, L., Eilbeck, J., Marn, J., and Russell, F. (2000). Breathers in systems with intrinsic and extrinsic nonlinearities. *Physica D*, **142**(1-2), 101–112.

[31] Cruzeiro-Hansson, L., Eilbeck, J., Marn, J., and Russell, F. (2004). Dynamical two electron states in a Hubbard-Davydov model. *Eur. Phys. J. B*, **42**, 95–102.

[32] Cuevas, J., Kevrekidis, P., Frantzeskakis, D., and Bishop, A. (2008). Existence of bound states of a polaron with a breather in soft potentials. *Phys. Rev. B*, **74**(6), 064304.

[33] Davydov, A. S. (1973). The Theory of Contraction of Proteins under their Excitation. *J. Theor. Biol.*, **38**, 559–569.

[34] Davydov, A. S. (1977). Solitons and Energy Transfer Along Protein Molecules. *J. Theor. Biol.*, **66**, 379–387.

[35] Davydov, A. S. (1980). Soliton motion in a one-dimensional molecular lattice with account taken of thermal oscillations. *Sov. Phys. JETP*, **51**(2), 397–400.

[36] Davydov, A. S. (1982). *Biology and Quantum Mechanics*. Pergamon Press.

[37] Davydov, A. S. (1986). Quantum Theory of the Motion of Quasi-Particle in a Molecular Chain with Thermal Vibrations Taken into Account. *Phys. Stat. Sol. b*, **138**, 559–576.

[38] Edler, J. and Hamm, P. (2002). Self-trapping of the amide I band in a peptide model crystal. *J. Chem. Phys.*, **117**(5), 2415.

[39] Edler, J. and Hamm, P. (2003). Two-dimensional vibrational spectroscopy of the amide I band of crystalline acetanilide: Fermi resonance, conformational substates, or vibrational self-trapping? *J. Chem. Phys.*, **119**(5), 2709.

[40] Edler, J. and Hamm, P. (2004). Spectral response of crystalline acetanilide and N - methylacetamide: Vibrational self-trapping in hydrogen-bonded crystals. *Phys. Rev. B*, **69**(21), 214301.

[41] Eilbeck, J. C., Lomdahl, P. S., and Scott, A. C. (1984). Soliton structure in crystalline acetanilide. *Phys. Rev. B*, **30**, 4703–4712.

[42] Falvo, C. and Pouthier, V. (2005a). Vibron-polaron in -helices. i. single-vibron states. *J. Chem. Phys.*, **123**(18), 184709.

[43] Falvo, C. and Pouthier, V. (2005b). Vibron-polaron in -helices. ii. two-vibron bound states. *J. Chem. Phys.*, **123**(18), 184710.

[44] Fidder, H., Knoester, J., and Wiersma, D. A. (1991). Optical-Properties Of Disordered Molecular Aggregates - A Numerical Study. *J. Chem. Phys.*, **95**(11), 7880–7890.

[45] Flach, S. and Gorbach, A. V. (2008). Discrete breathers - Advances in theory and applications. *Phys. Rep.*, **467**(1-3), 1–116.

[46] Franco, M., Turin, L., Mershin, A., and Skoulakis, E. (2011). Molecular vibration-sensing component in Drosophila melanogaster olfaction. *Proc. Nat. Acad. Sci. U.S.A*, **108**, 3797–3802.

[47] Freedman, H., Martel, P., and Cruzeiro, L. (2010). Mixed quantum-classical dynamics of an amide i vibrational excitation in a protein α-helix. *Phys. Rev. B*, **82**, 174308.

[48] Freedman, H., Laino, T., and Curioni, A. (2012). Reaction Dynamics of ATP Hydrolysis in Actin Determined by ab lnitio Molecular Dynamics Simulations. *JCTC*, **8**(9), 3373–3383.

[49] Gerstein, M. and Krebs, W. (1998). A database of macromolecular motions. *Nuc. Acid. Res.*, **26**(18), 4280–4290.

[50] Gerstein, M. and Krebs, W. (2006). The Database of Macromolecular Motions: new features added at the decade mark. *Nuc. Acid. Res.*, **34**, D296D301.

[51] Hamm, P. (2009). Femtosecond IR Pump-Probe Spectroscopy of Nonlinear Energy Localization in Protein Models and Model Proteins. *J. Biol. Phys.*, **35**(1), 17–30.

[52] Harel, E. and Engel, G. (2012). Quantum coherence spectroscopy reveals complex dynamics in bacterial light-harvesting complex 2 (LH2). *Proc. Nat. Acad. Sci. U.S.A*, **109**(3), 706–711.

[53] Holstein, T. (1959a). Studies of polaron motion: Part I. The Molecular Crystal Model. *Ann. Phys.*, **8**, 325–342.

[54] Holstein, T. (1959b). Studies of polaron motion: Part II. The "small" polaron. *Ann. Phys.*, **8**, 343.

[55] Hub, J. and de Groot, B. (2009). Detection of Functional Modes in Protein Dynamics. *PLOS Computat. Biol.*, **5**(8), e1000480.

[56] Huelga, S. and Plenio, M. (2013). Vibrations, quanta and biology. *Contemporary Phys.*, **54**(4), 181–207.

[57] Hyman, J. M., McLaughlin, D. W., and Scott, A. C. (1981). On Davydov's alpha-helix solitons. *Physica D*, **3**(1-2), 23–44.

[58] Ichiye, T. and Karplus, M. (1991). Collective Motions In Proteins - A Covariance Analysis Of Atomic Fluctuations In Molecular-Dynamics And Normal Mode Simulations. *Proteins-Struc. Func. Gen.*, **11**(3), 205–217.

[59] Kenkre, V. M. and Grigolini, P. (1993). A New Nonlinear Stochastic Liouville Equation: Inclusion of Finite Relaxation and Finite Temperature Effects. *Z. Phys. B*, **90**, 247–253.

[60] Lawrence, A. F., McDaniel, J. C., Chang, D. B., Pierce, B. M., and Birge, R. R. (1986). Dynamics of the Davydov model in α-helical proteins: Effects of the coupling parameter and temperature. *Phys. Rev. A*, **33**(2), 1188–1201.

[61] Lawrence, A. F., McDaniel, J. C., Chang, D. B., , and Birge, R. R. (1987). The Nature of Phonons and solitary waves in α-helical proteins. *Biophys. J.*, **51**, 785–793.

[62] Lindblad, G. (1976). On the Generators of Quantum dynamical semigroups. *Comm. Math. Phys.*, **48**, 119–119.

[63] Lomdahl, P. S. and Kerr, W. C. (1985). Do Davydov Solitons Exist at 300 K? *Phys. Rev. Lett.*, **55**(11), 1235–1238.

[64] M, C., PH, H., D, B., R, B., R, B., DP, G., TN, H., MA, K., V, K., C, O., C, P., D, T., and van Gunsteren WF (2005). The gromos software for biomolecular simulation: Gromos05. *J. Computat. Chem.*, **26**(16), 1719–1751.

[65] MacKay, R. S. and Aubry, S. (1994). Proof of Existence of Breathers for Time-Reversible or Hamiltonian Networks of Weakly Coupled Oscillators. *Nonlinearity*, **7**, 1623–1643.

[66] MacNeil, L. and Scott, A. C. (1984). Launching a Davydov soliton: II. Numerical Studies. *Phys. Scr.*, **29**, 284–287.

[67] Mahajan, S. and Sanejouand, Y. (2015). On the relationship between low-frequency normal modes and the large-scale conformational changes of proteins. *Arch. Biochem. Biophys.*, **567**, 59–65.

[68] Mauri, F., Car, R., and Tosatti, E. (1993). Canonical Statistical Averages of Coupled Quantum-Classical Systems. *Europhys. Lett.*, **24**(6), 431–436.

[69] McClare, C. (1974). Resonance in bioenergetics. *Ann. N. Y. Acad. Sci.*, **227**, 74–97.

[70] Morales, M. (1974). General Discussion. *Ann. N. Y. Acad. Sci.*, **227**, 108–115.

[71] Nicolay, S. and Sanejouand, Y. (2006). Functional modes of proteins are among the most robust. *Phys. Rev. Lett.*, **96**(7), 078104.

[72] Nosé, S. (1984). A Molecular Dynamics Method for Simulations in the Canonical Ensemble. *Mol. Phys.*, **52**, 255–268.

[73] Panitchayangkoon, G., Hayes, D., Fransted, K., Caram, J., Harel, E., Wen, J., Blankenship, R., and Engel, G. (2010). Long-lived quantum coherence in photosynthetic complexes at physiological temperature. *Proc. Nat. Acad. Sci. U.S.A*, **107**(29), 12766–12770.

[74] Panitchayangkoon, G., Voronine, D., Abramavicius, D., Caram, J., Lewis, N., Mukamel, S., and Engel, G. (2011). Direct evidence of quantum transport in photosynthetic light-harvesting complexes. *Proc. Nat. Acad. Sci. U.S.A*, **108**(52), 20908–20912.

[75] Percival, I. (1998). *Quantum State Diffusion*. Cambridge University Press.

[76] Pouthier, V. (2007). Two-site realization of the davydov model in a finite size lattice: A time-convolutionless master equation approach. *Phys. Rev. E*, **75**, 061910.

[77] Pouthier, V. (2008a). Amide-I lifetime-limited vibrational energy flow in a one-dimensional lattice of hydrogen-bonded peptide units. *Phys. Rev. E*, **78**(6), 061909.

[78] Pouthier, V. (2008b). Energy relaxation of the amide-I mode in hydrogen-bonded peptide units: A route to conformational change. *J. Chem. Phys.*, **128**(6), 065101.

[79] Press, William H. Flannery, B. P., Teukolsky, S. A., and Vetterling, W. T. (1986). *Numerical Recipes: The Art of Scientific Computing*. Cambridge University Press.

[80] Ritz, T., Thalau, P., Phillips, J., Wilschko, R., and Wilschko, W. (2004). Resonance effects indicate a radical-pair mechanism for avian magnetic compass. *Nature*, **429**, 177–180.

[81] Schmidt, J. R., Parandekar, P. V., and Tully, J. C. (2008). Mixed quantum-classical equilibrium: Surface hopping. *J. Chem. Phys.*, **129**, 044104.

[82] Scott, A. (1992). Davydov's soliton. *Phys. Rep.*, **777**, 1–68.

[83] Scott, A. C. (1982). Dynamics of Davydov solitons. *Phys. Rev. A*, **26**(1), 578–595.

[84] Scott, A. C. (1984). Launching a Davydov soliton: I. Soliton Analysis. *Phys. Scr.*, **29**, 279–283.

[85] Scott, A. C., Bigio, I. J., and Johnston, C. T. (1989). Polarons in acetanilide. *Phys. Rev. B*, **39**, 12883–12887.

[86] Sievers, A. J. and Takeno, S. (1988). Intrinsic Localized Modes in Anharmonic Crystals. *Phys. Rev. Lett.*, **61**(8), 970–973.

[87] Silva, P. and Cruzeiro, L. (2006). Dynamics of a nonconserving Davydov monomer. *Phys. Rev. E*, **74**, 021920.

[88] Silva, P. and Cruzeiro-Hansson, L. (2003). A reduced set of exact equations of motion for a non-number-conserving Hamiltonian. *Phys. Lett. A*, **315**, 447–451.

[89] Springborg, M. (2000). *Methods of Electronic-Structure Calculations. From Molecules to Solids*. John Wiley & Sons, Chichester-Toronto, first edition.

[90] Turin, L. (1996). A spectroscopic mechanism for primary olfactory reception. *Chem. Sens.*, **21**, 773–791.

[91] Turin, L. (2009). Colin McClare (1937-1977): a tribute. *J. Biol. Phys.*, **35**, 1–7.

[92] Turin, L., Skoulakis, E., and Horsfield, A. (2014). Electron spin changes during general anesthesia in Drosophila. *Proc. Nat. Acad. Sci. U.S.A*, **111**(34), E3524–E3533.

[93] Wang, W., Bishop, A., Gammel, J., and RN, S. (1998). Quantum breathers in electronphonon systems. *Phys. Rev. Lett.*, **80**, 3284–3287.

[94] Wang, X., Brown, D., and Lindenberg, K. (1988). Alternative Formulation Of Davydov Theory Of Energy-Transport In Biomolecular Systems. *Phys. Rev. A*, **37**(9), 3557–3566.

[95] Wang, X., Brown, D., and Lindenberg, K. (1989). Quantum Monte-Carlo Simulation Of The Davydov Model. *Phys. Rev. Lett.*, **62**(15), 1796–1799.

[96] Xie, A., van der Meer, L., Hoff, W., and Austin, R. H. (2000). Long-lived amide i vibrational modes in myoglobin. *Phys. Rev. Lett.*, **84**, 5435–5438.

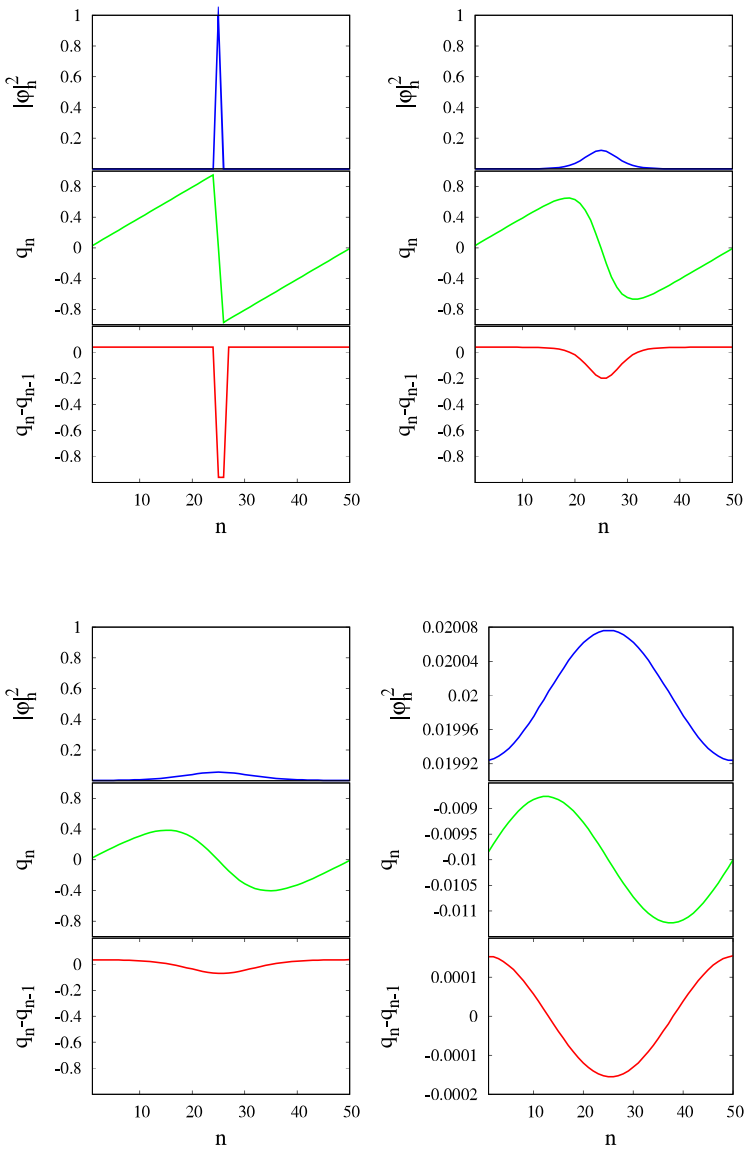

FIG. 1. (Colour online) Minimum energy states as a function of v (see 10), for $N = 50$. Top right: $v = 0$; Top left: $v = -4$; Bottom right: $v = -8$; Bottom left: $v = -10.30$. In each panel the top plot (blue) displays the probability amplitude for the amide I excitation to be in lattice site n, $|\phi_n|^2$, the middle plot (green) displays the actual displacements of each laticce site q_n, and the bottom plot (red) displays the displacement differences $(q_n - q_{n-1})$.

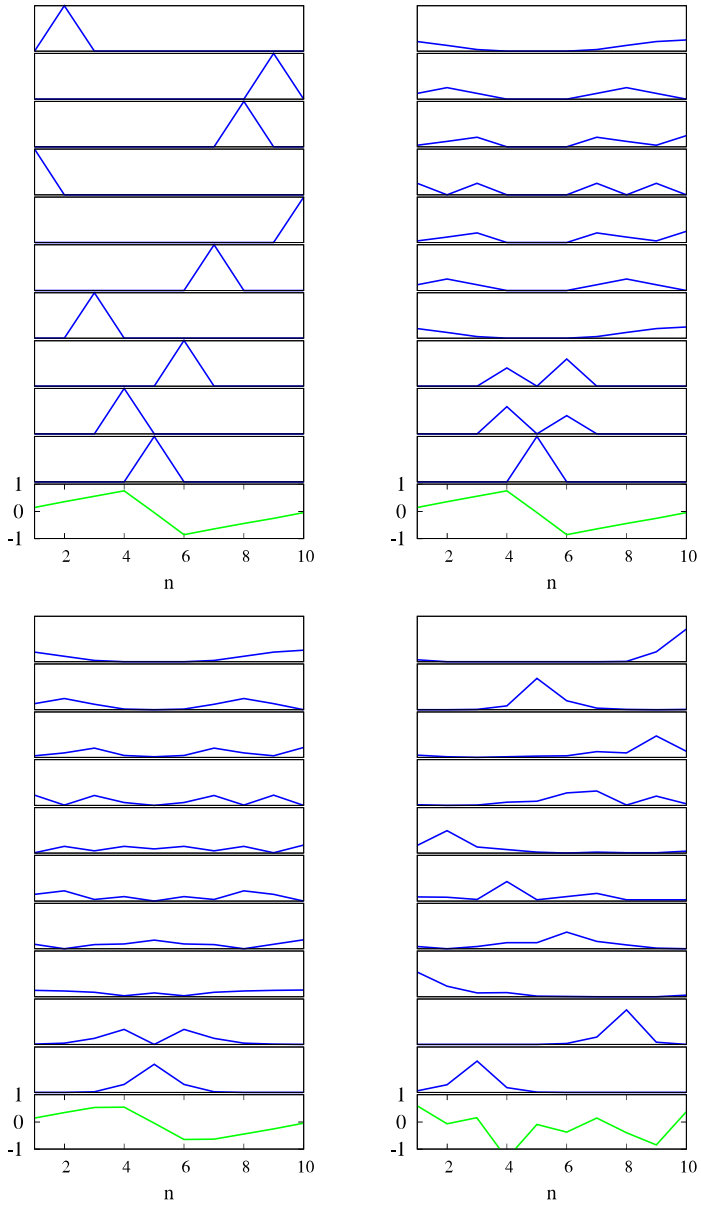

FIG. 2. (Colour online) Full band of amide I states for lattice distortion of minimum energy solution with $v = 0$ (top right panel), $v = -0.000001$ (top left panel); $v = -0.54$ (bottom right panel) and for a disordered lattice at $T = 0.5$ and $v = -0.54$ (bottom left panel). In each panel, the lowest plot is the lattice configuration and the next plots are the amide I eigenstates for that lattice configuration, with energy increasing from bottom to top.

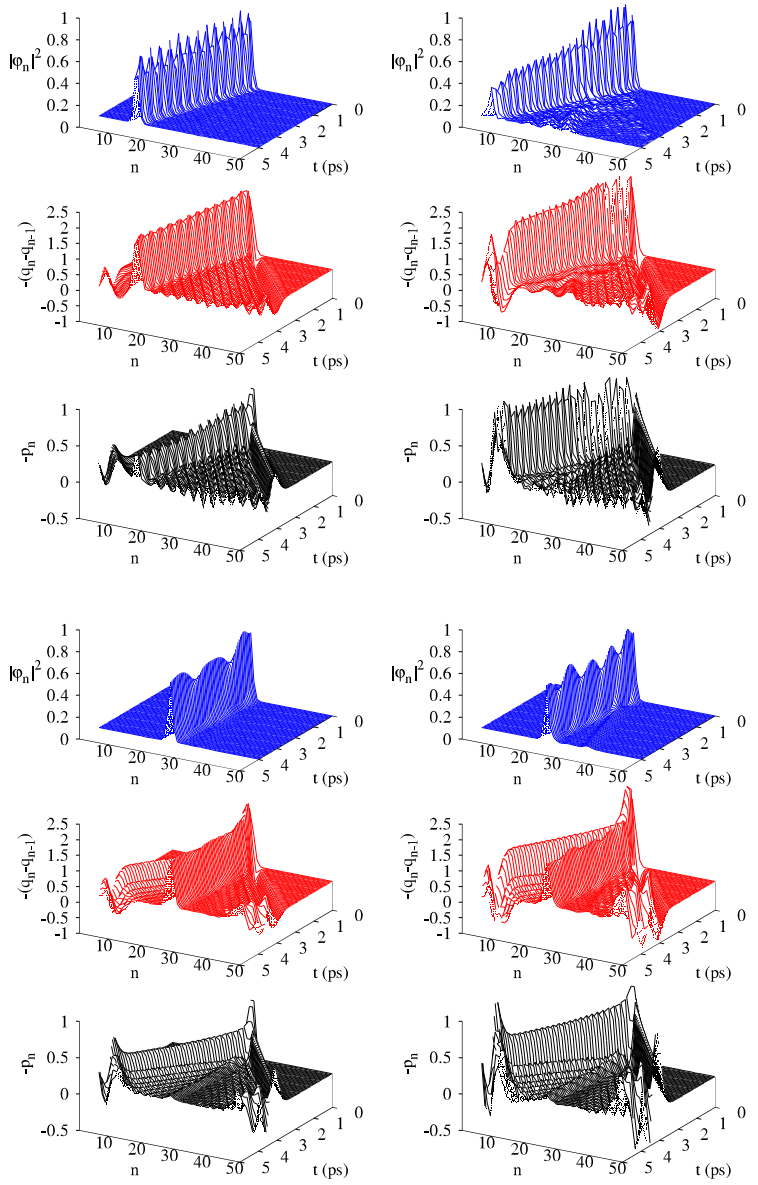

FIG. 3. (Colour online) Short time dynamical evolution a velocity driven minimum energy state obtained with $v = -0.54$. Top right: $m = 0.45$, $A = 1$; Top left: $m = 0.45$, $A = 2$; Bottom right: $m = 3$, $A = 1$; Bottom left: $m = 3$, $A = 2$. (11-12) have been used.

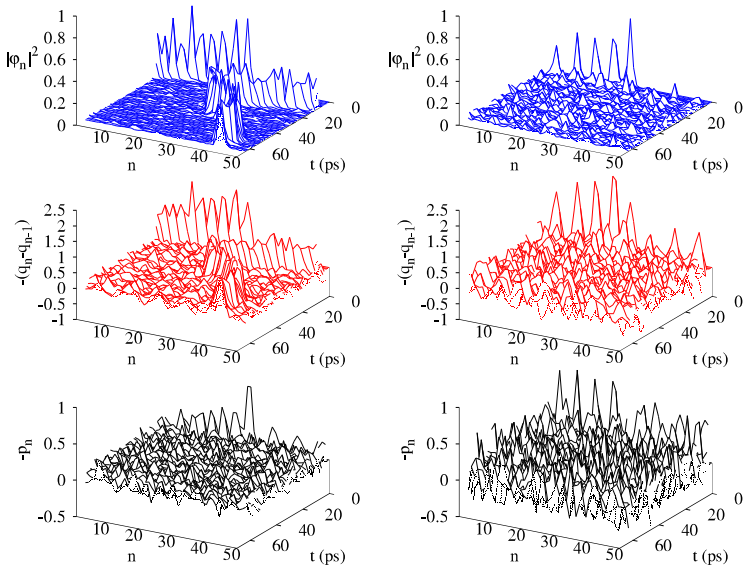

FIG. 4. (Colour online) Long time dynamical evolution a velocity driven minimum energy state obtained with $v = -0.54$, $m = 0.45$. $A = 1$ (left) and $A = 2$ (right).

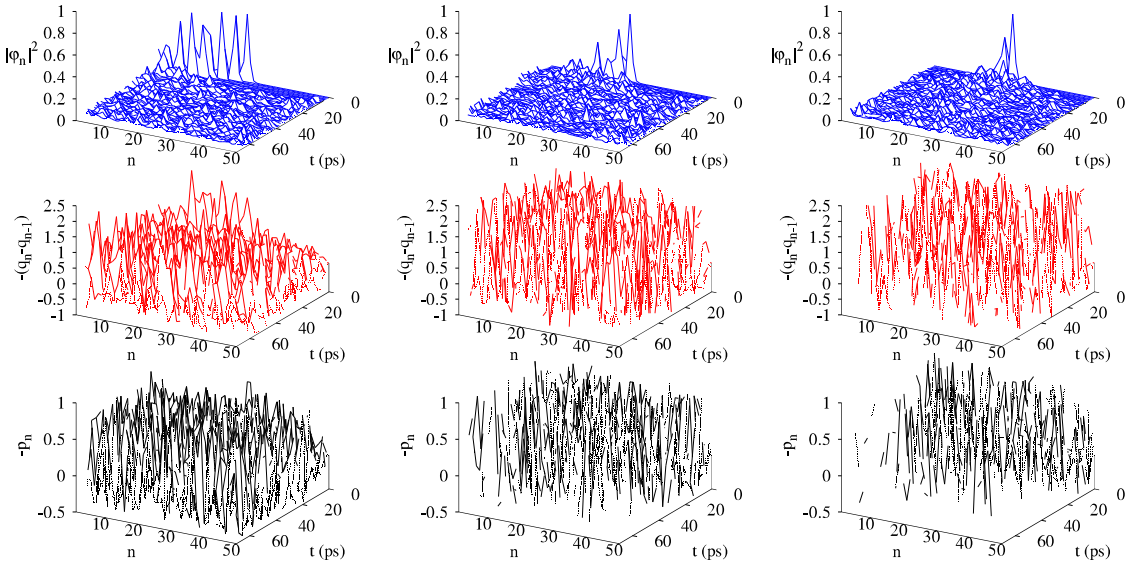

FIG. 5. (Colour online) Time evolution of a velocity driven minimum energy state at $T = 0.5$ (left), $T = 5$ (middle) and $T = 14$ (bottom). Other parameters are: $v = -0.54$, $m = 0.45$, $A = 1$.Eqs.(17-18) have been used.

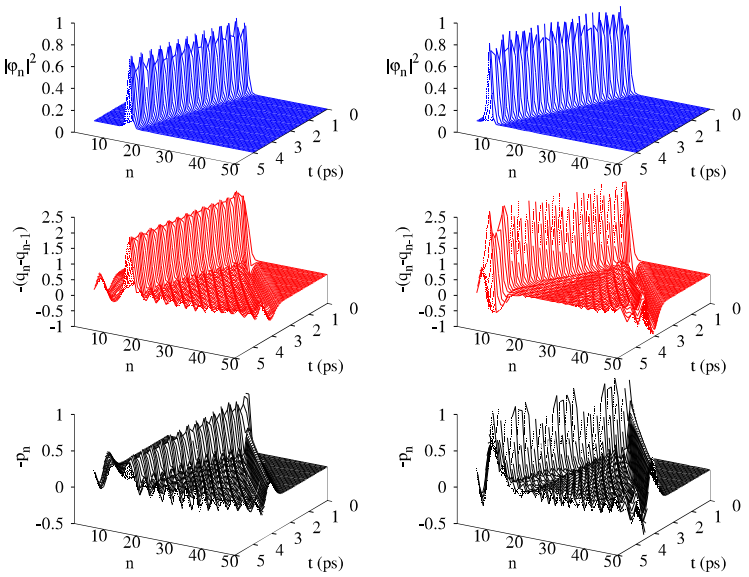

FIG. 6. (Colour online) Time evolution of a velocity driven minimum energy state for $A = 1$ (left) and $A = 2$ (right). Other parameters are: $v = -0.54$ and $T = 0$. Eqs.(22-23) have been used.

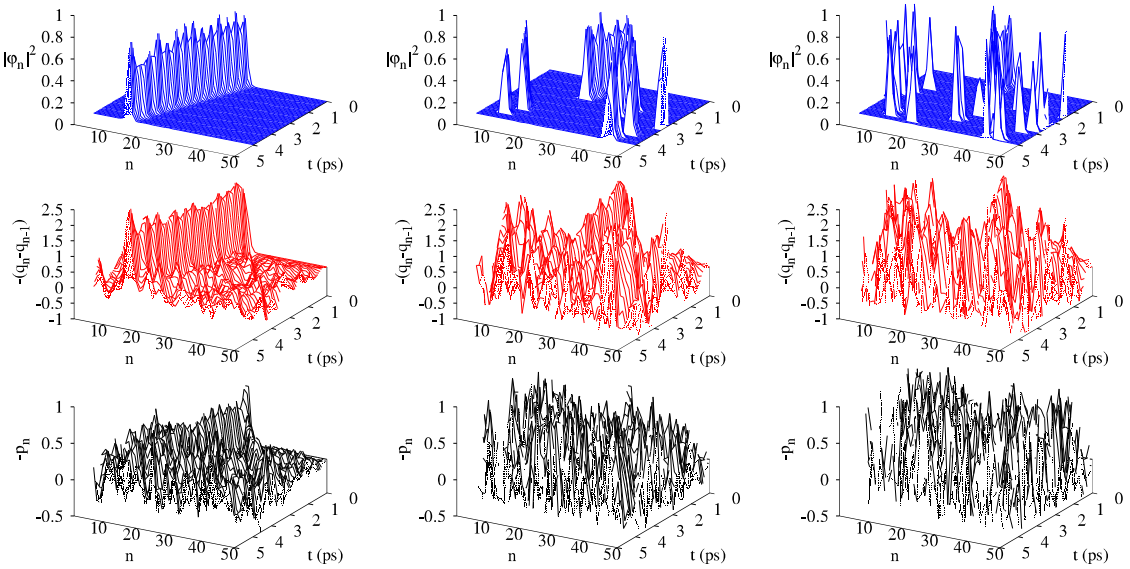

FIG. 7. (Colour online) Time evolution of a velocity driven minimum energy state for $T = 0.5$ (left), $T = 5.0$ (middle) and $T = 14$ (right). Other parameters are: $v = -0.54$ and $A = 1$. Eqs.(22-23) have been used.

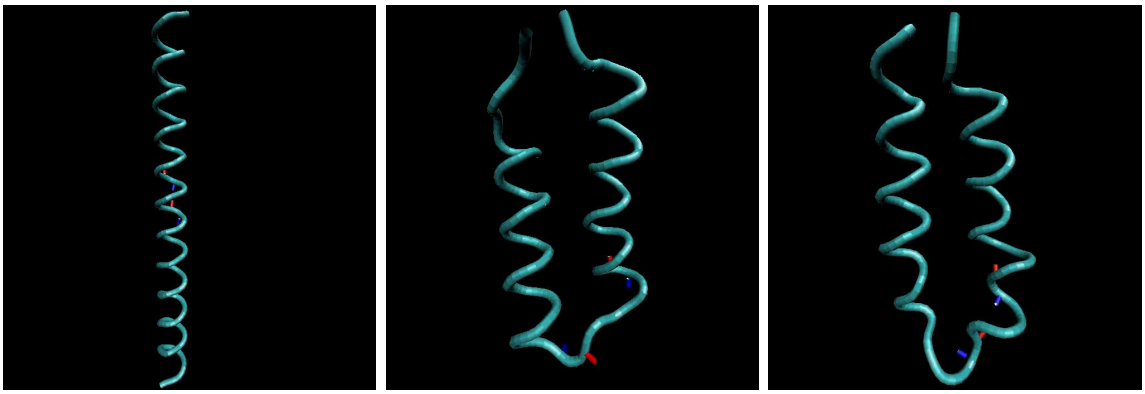

FIG. 8. (Colour online) The initial conformation of the protein is an alpha helix (left panel). The target conformation is the native structure (middle panel). The best final conformation achieved after many trials (right panel). The C=O and H-N groups where particular initial momenta were added initially (see text) are displayed as thick bonds in red and blue, respectively.

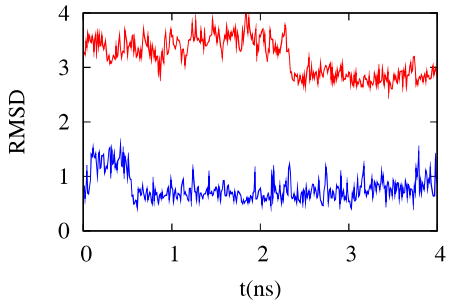

FIG. 9. (Colour online) RMSD of each structure in the trajectory with respect to the average structure in that trajectory for the native state (blue, bottom curve) and for the alternative structure (red, top curve), in the last 4 nanoseconds of a 40 nanosecond simulation.

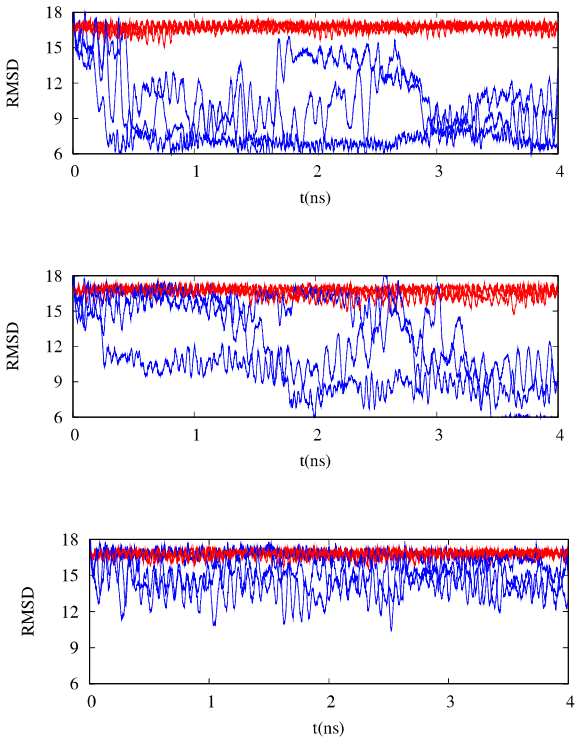

FIG. 10. (Colour online) RMSD of each structure in the trajectory with respect to the native state in the presence of initial velocities in atoms C=O(amino acid 21)...H-N-C=O(amino acid 25)...H-N(amino acid 29) (blue curves) and in their absence (red curves).